Theoretical investigation of a Ge 2D photonic crystal by optical reflectivity correlated with band distributions

D. G. POPESCU*
National Institute of Materials Physics, Atomistilor 105b, 077125 Magurele-Ilfov, Romania

A two dimensional photonic crystal with hexagonal symmetry is investigated by finite-difference time-domain and finite-difference frequency-domain theoretical calculations. The system consist in a germanium substrate patterned with holes of different radii, varying from $0.1a$ to $0.45a$. The photonic band gaps (PBGs) and the reflectance spectra allow a complete characterization of the structure. It was shown the presence of PBGs at telecommunication wavelengths which makes the present systems suitable for optoelectronic applications, representing a potential alternative to Si-based technology

(Received September 1, 2015; accepted September 29, 2016)

Keywords: FDTD analyses, Photonic band gaps, Reflectivity

1. Introduction

In the last decades, many researchers have been devoted to the study of Photonic Crystals (PhCs) [1 - 10] in all of the three dimensions. These systems, which allow the manipulation of light at wavelength scale, display forbidden frequency region. These domains, where the propagation of light waves is strictly forbidden, are called photonic band gaps (PBGs) or Stop-Gaps. The importance of PBGs is associated with the possibility of designing ultra-compact photonic integrated circuits, permitting light diffraction in UV, visible and near infrared, better confinement of light in ultra-small spaces and high speed of operation. Optical filters [11], waveguides [4, 9], PhC fibers [12], optical switches [13, 14] are some examples of optical devices based on these periodic dielectric structures. The PBGs can be manipulated by modeling the refractive index, lattice constant and sample thickness. Furthermore, a key factor is their dispersion diagrams, characterized by photonic mode energies for different photonic crystal designs. Due to their scalability is easier to study two-dimensional (2D) PhCs rather than three-dimensional ones. It is known that silicon has been established as the material of choice for industry. Nevertheless in photonics it presents constrains regarding its indirect bandgap and the limited degree of freedom in material design. On the other hand, the device miniaturization on high dielectric systems made possible the replacement of Si as channel material, germanium (Ge) offering the advantage of direct CMOS compatibility [15], a low dispersion properties in a wide range of temperatures and a higher refractive index ($n\sim4.2$). Additionally, Ge is an excellent photodetector material for applications in on-chip data distribution [16], solar cells [17], lasers [18] and as well for emitters [19].

In this paper we investigate the properties of 2D PhCs, exploring the feasibility of using Ge as a substrate for applications in photonics. The hexagonal symmetry was considered in order to explain the experimental results [20-23]. The calculations were performed using the finite-difference time-domain (FDTD), for computing reflectivity spectra, and the finite-difference frequency-domain (FDFD), for band gap and field patterns calculations. The paper is organized as follows: in Section 2 a brief description of the numerical method is given. In sections 3 and 4 the dispersion laws and reflectance spectra are calculated, with a special emphasis on the effects of fundamental parameters on the photonic band gap of the system and Section 5 is dedicated to potential applications and conclusions of the paper.

2. Numerical methods

In order to design PhC – based devices it is important to take into account the band structure of these artificially created materials and to obtain the most suitable PBG with respect to our operational wavelength. Presently, the best ways for analyzing the band structure and achieving the photonic band gaps in our photonic structures are numerical methods. One of the most used techniques is FDFD method [24]. MIT Photonic Bands (MPB) Package, as well as MIT Electromagnetic Equation Propagation (MEEP) [25], used for reflectance spectra, provide very accurate prediction and characterization of the properties of propagating photons.

MPB computes directly eigenstates and eigenvalues of the Maxwell equations (1) in the frequency domain [26]:

$$\nabla \times \left(\frac{1}{\varepsilon(\mathbf{r})}\nabla \times \mathbf{H}(\mathbf{r})\right) = \left(\frac{\omega}{c}\right)^2 \mathbf{H}(\mathbf{r}) \qquad (1)$$

with $\varepsilon(r)$ – the dielectric function, c – the speed of light in vacuum, $\left(\frac{\omega}{c}\right)^2$ – the eigenvalue. The periodicity of $\varepsilon(r)$ allow the expansion of both magnetic field $\mathbf{H}(\mathbf{r})$ and $\varepsilon(r)$ in terms of plane waves [27] using Bloch's theorem.

It prevents step discontinuities by Fourier transform over an infinite repetition of the computational cell into all directions. MPB can calculate the guided modes (strong localized ones) at high precision, the weak ones (leaky modes) being dependent on the period introduced in vertical direction. This shortcoming may be overcome by choosing a computational cell in vertical direction comparable with a few times the lattice constants. The advantage of the MPB is the accuracy of band structures and eigenstates calculations.

MEEP is a FDTD code applied in modeling electromagnetic systems. It allows the transmission or scattering spectra calculations in finite structure [26]. It can be used to handle 2D and 3D photonic structures, like photonic crystals, and other optical systems.

Within the theoretical computations MEEP calculates the propagation of fields directly as a function of space and time, using Maxwell's equations. However, it is necessary to specify light sources and flux planes.

One can investigate with MEEP multiple electromagnetic situations with the possibility of pictures or movies production. Transmission and reflection spectra can be computed by a single calculations followed by a Fourier-transformation as a response to a short pulse emitted by the source. It is necessary to run the program twice, the first one for an empty space, and the second one for the studied geometry. The final flux is obtained dividing the reflection by the reference flux.

3. Photonic Band Gap Calculations

The first step in designing two-dimensional photonic crystals in germanium is to calculate the band structure and to obtain the most suitable photonic band gap. In our case a Ge matrix of permittivity $\varepsilon=16.2$ was used. Due to the fact that the imaginary part of the dielectric constant does not affect the dispersion relation of a regular structure within this paper it is assumed to be zero. Additionally, the reflectance spectra for the considered structure are calculated in order to study the effects which appear at the surface.

The dispersion relations of our structure with values for the refractive index given below are shown in Figures 1 – 7. The dispersion laws of the PhC structure consisting in air cylinders with $R = 0.10a$ lacks the gaps, therefore they were not illustrated. The images of the 2D PhC system under study are depicted in the insets of the figures. Germanium provides the large in-plane refractive index contrast, higher than 3, which is required for a strong band gaps effect and guided mode experiences. The radii of the cylinders were varied from $R = 0.10a$ to $R = 0.45a$, where $a = 1.5\,\mu m$ represents the lattice constant. Thirty bands were computed at a 32 resolution. The frequencies are expressed in c/a units, with c the speed of light.

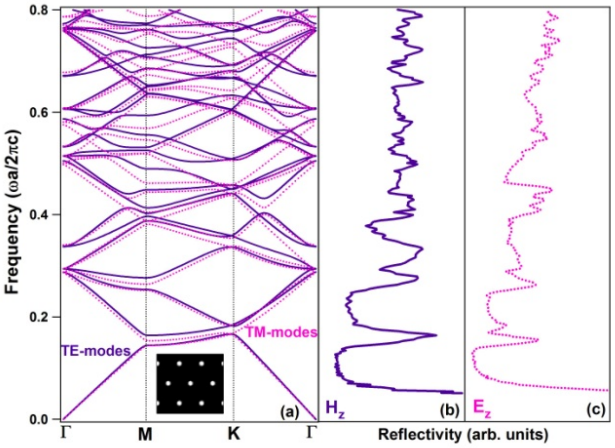

Fig. 1. (a) Computed dispersion laws of a 2D triangular PhC structure consisting in air cylinders with $R = 0.15a$, where $a = 1.5\,\mu m$ is the lattice constant, in Ge matrix for TE modes (continuous line) and TM modes (dashed line). Inset: PhC system; (b) and (c) theoretical reflectivity spectra in Γ direction calculated using H_z and E_z fields.

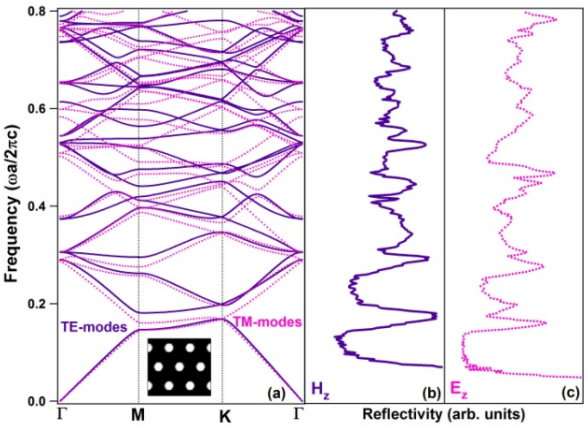

Fig. 2. (a) Computed dispersion laws of a 2D triangular PhC structure consisting in air cylinders with R = 0.20a, where a = 1.5μm is the lattice constant, in Ge matrix for TE modes (continuous line) and TM modes (dashed line). Inset: PhC system; (b) and (c) theoretical reflectivity spectra in Γ direction calculated using H_z and E_z fields.

Using these specifications the photonic band gaps, the reflectivity, the magnetic and electric field distribution were calculated. Thereby, the parameters were chosen to examine the imaging properties of the 2D photonic systems at near-infrared frequency regime.

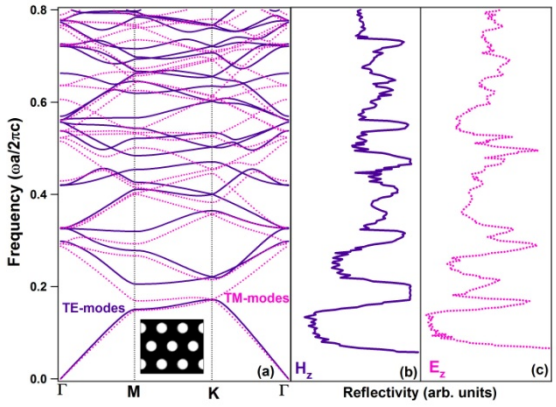

Fig. 3. (a) Computed dispersion laws of a 2D triangular PhC structure consisting in air cylinders with R=0.25a, where a=1.5μm is the lattice constant, in Ge matrix for TE modes (continuous line) and TM modes (dashed line). Inset: PhC system; (b) and (c) theoretical reflectivity spectra in Γ direction calculated using H_z and E_z fields.

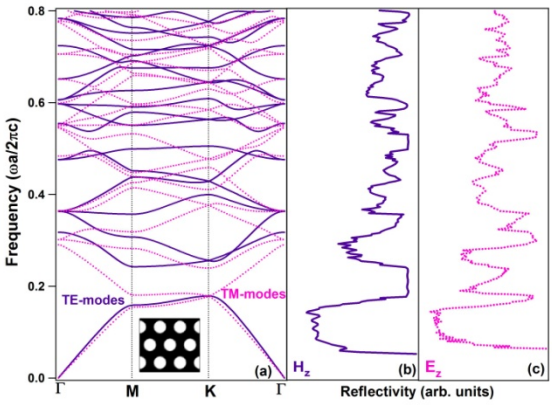

Fig. 4. (a) Computed dispersion laws of a 2D triangular PhC structure consisting in air cylinders with R=0.30a, where a=1.5μm is the lattice constant, in Ge matrix for TE modes (continuous line) and TM modes (dashed line). Inset: PhC system; (b) and (c) theoretical reflectivity spectra in Γ direction calculated using H_z and E_z fields.

The band gap diagrams gather the computed TE and TM modes as a function of wavenumber *k* ranging from Γ point to M and K. The corresponding reflectance spectra are associated with the dispersion diagrams, with maximum reflectance in the gaps (the photons with energy in the gap do not propagate) and minimum one outside the gaps.

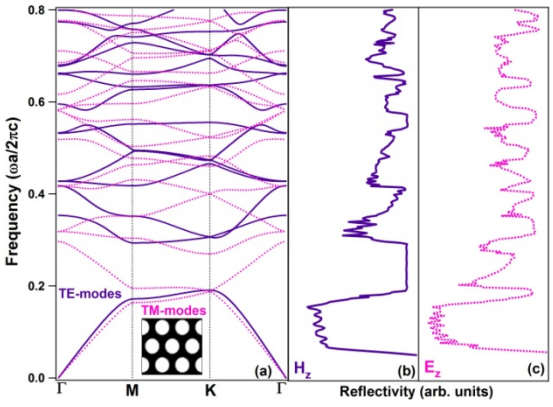

Fig. 5. (a) Computed dispersion laws of a 2D triangular PhC structure consisting in air cylinders with R=0.35a, where a=1.5μm is the lattice constant, in Ge matrix for TE modes (continuous line) and TM modes (dashed line). Inset: PhC system; (b) and (c) theoretical reflectivity spectra in Γ direction calculated using H_z and E_z fields.

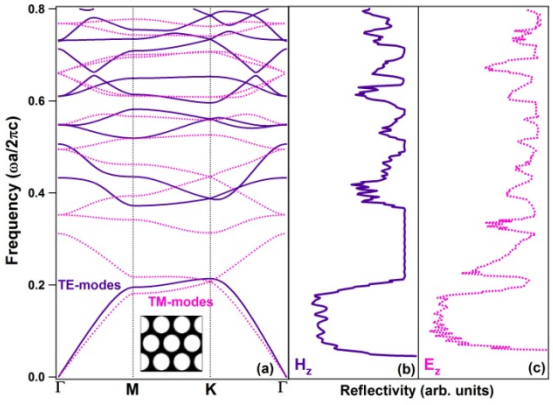

Fig. 6. (a) Computed dispersion laws of a 2D triangular PhC structure consisting in air cylinders with R=0.40a, where a=1.5μm is the lattice constant, in Ge matrix for TE modes (continuous line) and TM modes (dashed line). Inset: PhC system; (b) and (c) theoretical reflectivity spectra in Γ direction calculated using H_z and E_z fields.

The air-filling factors for our tested structures [28], calculated with equation (2), are displayed in Table I:

$$f = \frac{\pi R^2}{a^2} \tag{2}$$

Table I: The air-filling factors for different radii varying from R=0.10a to R=0.45a, in the case of lattice constant a=1.5μm.

R	0.10	0.15	0.20	0.25	0.30	0.35	0.40	0.45
f	3.1	7.1	12.1	19.6	28.3	38.45	50.2	63.6

A close inspection of the dispersion bands reveals the presence of at most 4 bandgaps in the TE modes case and 5 for the TM ones. The detailed list comprising the existence of these gaps is provided in Table II. The largest ones are present between the first and the second TE mode bands, with a relative bandgap width $\eta = \frac{\Delta\omega}{\omega}$ ranging from $\eta = 7.316\,\%\ (R = 0.20a)$ to $\eta = 57.325\%\ (R = 0.45a)$, where $\Delta\omega$ represents the bandgap widths and ω the central frequency.

In the TM modes case, the band gap relative width extends from $\eta = 0.538\%\ (R = 0.40a)$ to $\eta = 11.329\%\ (R = 0.45a)$. Furthermore, some complete gaps for both TE and TM modes can be observed ranging from 0.582 to 0.596, from 0.312 to 0.313 and from 0.347 to 0.389 frequency intervals.

The most feasible systems are the PhCs having $R = 0.40a$ and $R = 0.45a$, which possess a gap at $1.5\ \mu m$ frequency and $1.3\ \mu m$,

respectively for transversal electric modes in the telecommunications frequency range. This may represent an important opportunity for designing coupled cavities based applications, improving the present Si-technology.

In the reflectance spectra (Figs. 1 – 7 (b) and (c)) the signature of some partial gaps near the center of the Brillouin zone can also be seen.

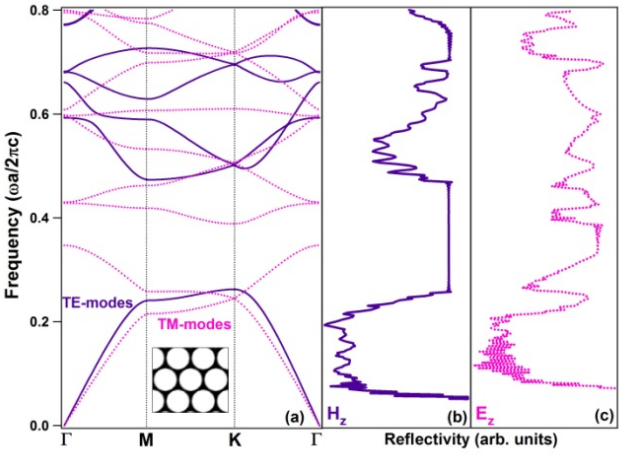

Fig. 7. (a) Computed dispersion laws of a 2D triangular PhC structure consisting in air cylinders with R=0.45a, where a=1.5 μm is the lattice constant, in Ge matrix for TE modes (continuous line) and TM modes (dashed line). Inset: PhC system; (b) and (c) theoretical reflectivity spectra in Γ direction calculated using H_z and E_z fields.

Table 2: The band gaps for different radii varying from R=0.10a to R=0.45a, in the case of lattice constant a=1.5μm.

	Modes	Bands		Bands		η (%)
$R = 0.10a$	-	-	-	-	-	-
$R = 0.15a$	-	-	-	-	-	-
$R = 0.20a$	TE	B1	0.168	B2	0.181	7.316
$R = 0.25a$	TE	B1	0.172	B2	0.206	17.864
		B7	0.471	B8	0.484	2.831
		B10	0.557	B11	0.561	0.672
$R = 0.30a$	TE	B1	0.179	B2	0.243	30.259
		B7	0.505	B8	0.538	6.168
		B18	0.808	B19	0.815	0.819
$R = 0.35a$	TE	B1	0.191	B2	0.294	42.447
		B7	0.556	B8	0.582	4.712
		B20	0.935	B21	0.941	0.663
$R = 0.40a$	TE	B1	0.214	B2	0.372	54.174
		B3	0.506	B4	0.519	2.517
		B5	0.582	B6	0.596	2.388
		B7	0.655	B8	0.662	1.035
	TM	B2	0.312	B3	0.313	0.538
		B6	0.526	B7	0.549	4.220
		B7	0.571	B8	0.608	6.129
		B11	0.707	B12	0.741	4.687
		B13	0.778	B14	0.814	4.484
$R = 0.45a$	TE	B1	0.263	B2	0.473	57.325
		B5	0.727	B6	0.771	5.950
		B7	0.883	B8	0.898	1.744
		B17	1.259	B18	1.268	0.710
	TM	B2	0.347	B3	0.389	11.329
		B13	0.937	B14	0.956	2.034

The distributions of the magnetic field intensities for TE modes in the proximity of the high symmetry point Γ are given in Fig. 8. The analysis of the field patterns gives a deeper understanding of the photonic band gaps occurrence. The reflectivity spectra are in accordance with the interpretation derived from the band dispersion analysis. In Fig. 8 one can also observe how the field patterns changes for different resonance frequencies between upper and lower bands tuning the widths of the photonic band gaps. The frequencies for every point where the magnetic field patterns (see Fig. 8) have been computed are presented in Table III. Since the frequency of the Band 2 modes are lower than those of the Band 5 and 6, the modes for Band 2 are categorized as having "dielectric" band characteristics, while modes for Band 5 and 6 "air band" characteristics [20, 21, 29]. Such variation in the near-field distribution is connected to symmetry change. One can observe the migration of the second band from 0.288, in the $R = 0.15a$ case, at 0.593 for $R = 0.45a$. Similar phenomenon is present also for band 5 and 6. In the case of Band 2, the field distributions are classified as hexapolar modes. The ones found at Band 5 are classified as monopole and hexapolar modes, respectively. One can observe a large intensity of the magnetic field in the high dielectric index material in order to lower its frequency. Also, Band 6 modes are classified as bipolar (for $0.15a - 0.30a$ radii), decapolar (for $0.35a$ radius), octapolar (for $0.40a$ radius) and quadrupolar (for $0.45a$ radius) modes, respectively. Furthermore, concerning a periodic media consisting in holes in a dielectric structure it was observed [30] that the air region support high frequency states, while the dielectric ones the low frequency range. It is worth mentioning that the photonic band gaps became larger due to the difference in the field distribution as a consequence of increasing the dielectric constant in periodic systems, making from high index materials a suitable environment for designing photonic systems.

As a result, this structures could presumably cover a wide branch of applications from microwave to near-IR and visible domains.

Table 3: The frequency (in $\omega a/2\pi c$ units) in the proximity of Γ for every point where the magnetic field patterns were investigated. The radii were varied from $R = 0.15a$ to $R = 0.45a$, with $a = 1.5\ \mu m$ the lattice constant.

Radius	$0.15a$	$0.20a$	$0.25a$	$0.30a$	$0.35a$	$0.40a$	$0.45a$
Band 2	0.288	0.291	0.299	0.318	0.353	0.433	0.593
Band 5	0.294	0.307	0.328	0.364	0.428	0.549	0.682
Band 6	0.337	0.373	0.421	0.476	0.532	0.610	0.733

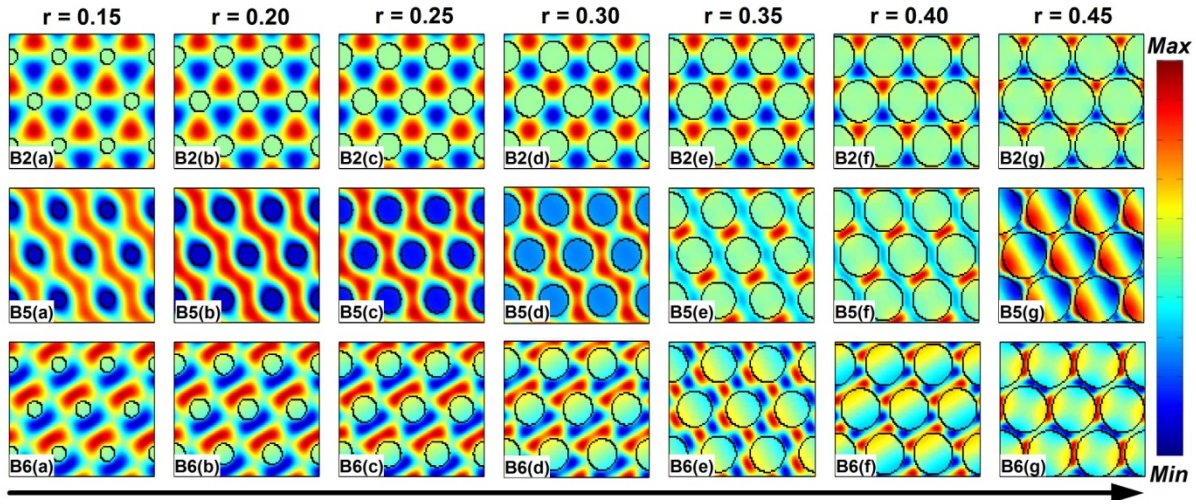

Fig. 8. Magnetic field distribution of transversal electric modes for 2, 5, and 6 bands, in the proximity of Γ point for the triangular lattice of PhC. The calculations are performed for different radii varying from R=0.15a to R=0.45a, with a=1.5μm. The colors indicate the amplitude of the magnetic field in the z direction.

4. Conclusions

A two-dimensional system with hexagonal symmetry consisting in holes in dielectric media was investigated through finite-difference time-domain and finite-difference frequency-domain simulations. The radii of the holes were varied from $R = 0.10a$ to $R = 0.45a$ in order to find a suitable configuration for future applications in telecommunication domain $1.3 - 1.5\ \mu m$. The lattice constant was fixed at $a = 1.5\ \mu m$ value, having in mind the scalability of the photonic systems.

This investigation permitted us to study the PBGs parameters which represent a map for PhCs classification. One could observe an increase in the gap at lower frequency (between Band 1 and Band 2) as the radius rose. This result proves the direct relation between the geometric parameters of the structure and its possibility to trap and guide the light in specific frequency range. The reflectance spectra offer the possibility of better understanding the optical properties for the studied systems.

In conclusion, FDFD and FDTD theoretical calculations, of photonic band structures, reflectance and magnetic field distributions, permit direct characterization of PhCs, which thus are proved as an alternative to Si-based technology in microphotonic structure fabrication, covering a wide branch of applications from microwave to near-IR and visible domains.

Acknowledgement

This work was financed by the Romanian UEFISCDI Agency under Contract PN 2 - Partnerships No. 152/2011.

References

[1] E. Yablonovitch, Phys. Rev. Lett. **58**, 2059 (1987) .
[2] S. John, Phys. Rev. Lett. **58**, 2486 (1987).
[3] S. Noda et al., Science **289**, 604 (2000).
[4] J.D. Joannopoulos et al., Photonic Crystals: Molding the Flow of Light, Princeton University Press, 2008
[5] A.M. Husanu, Phys. Status Solidi B **246**, 87 (2009).
[6] D.G. Popescu et al., J. Optoelectron. Adv. M. **15**, 610 (2013).
[7] X. Liu et al., Phys. Rev. Appl. **3**, 014006 (2015).
[8] H. Alipour-Banaei et al., J. Optoelectron. Adv. M. **17**, 259 (2015).
[9] U.W. Paetzold et al., Nano Lett. **14**, 6599 (2014).
[10] D.G. Popescu et al., J. Optoelectron. Adv. M. **14**, 356 (2012).
[11] Zheng Wang et al., Prhys. Rev. B **68**, 066616 (2003).
[12] D.G. Popescu et al., U.P.B. Sci. Bull., Series A **75**, 205 (2013).
[13] B. Rezaei et al., J. Mod. Optic. **61**, 904 (2014).
[14] F. Kaiser et al., New J. Phys. **14**, 085015 (2012).
[15] C.O.Chui, et al., Advanced Germanium MOS Devices. In Germanium-Based Technologies: from Materials to Devices Elsevier: Amsterdam, pp. 363, 2007.
[16] J. Michel et al., Nat. Photonics **4**, 527 (2010).
[17] V. Sorianello et al., Opt. Mater. Express **3**, 216 (2013).
[18] R.E. Camacho-Aguilera et al., Optics Express **20**, 11316 (2012).
[19] P. Boucaud et al., Photonics Res. **1**, 102 (2013).
[20] M.A. Husanu et al., Appl. Surf. Sci. **355**, 1186 (2015).
[21] M.A. Husanu et al., Eur. Phys. J. D **69**, 273 (2015)
[22] D.G. Popescu et al., Phys. Status Solidi RRL **7**, 274 (2013).
[23] D.G. Popescu et al., Thin Solid Films **552** 241 (2014)
[24] S. G. Johnson, J. D. Joannopoulos, The MIT Photonic-Bands Package (http://ab-initio.mit.edu/mpb/).
[25] S. G. Johnson, J. D. Joannopoulos, The MIT Electromagnetic Equation Propagation-Bands Package (http://ab-initio.mit.edu/meep/).
[26] S. Johnson et al., Opt. Express **8**, 173 (2001)
[27] Z. Zhang et al., Phys. Rev. Lett. **65**, 2650 (1990)
[28] A Cebrecos et al., J. Phys. D: Appl. Phys. **48**, 025501 (2014).
[29] K. Inoue et al., Photonic Crystals Springer-Verlag, 2004.
[30] L. Ondic et al., Appl. Phys. Lett. **102**, 251111 (2013)

*Corresponding author: dana.popescu@infim.ro